We are IntechOpen, the world's leading publisher of Open Access books
Built by scientists, for scientists

6,900
Open access books available

186,000
International authors and editors

200M
Downloads

Our authors are among the

154
Countries delivered to

TOP 1%
most cited scientists

12.2%
Contributors from top 500 universities

CLARIVATE ANALYTICS
BOOK CITATION INDEX
INDEXED

WEB OF SCIENCE™

Selection of our books indexed in the Book Citation Index
in Web of Science™ Core Collection (BKCI)

Interested in publishing with us?
Contact book.department@intechopen.com

Optical Coherence Tomography: Development and Applications

Anderson Zanardi de Freitas,
Marcello Magri Amaral and Marcus Paulo Raele
Nuclear and Energy Research Institute – IPEN-CNEN/SP
Brazil

1. Introduction

In early 90´s Huang *et al.*, applied the principles of low coherence interferometry to perform high resolution tomographic images of biological tissues. The technique became known as Optical Coherence Tomography (OCT) and opened new horizons in several areas of knowledge, e.g., ophthalmology (Hee, et al., 1995)(Meirelles, et al., 2005) and dermatology. In such areas other tomographic techniques does not reach resolutions good enough to study the structures of interest, see Fig. 1, in this way a whole new branch of imaging science was created. The OCT breakthrough was the capability of obtains high resolution histological images in vivo, in real time in non-invasive way and using harmless radiation (low power near infrared radiation, usually).
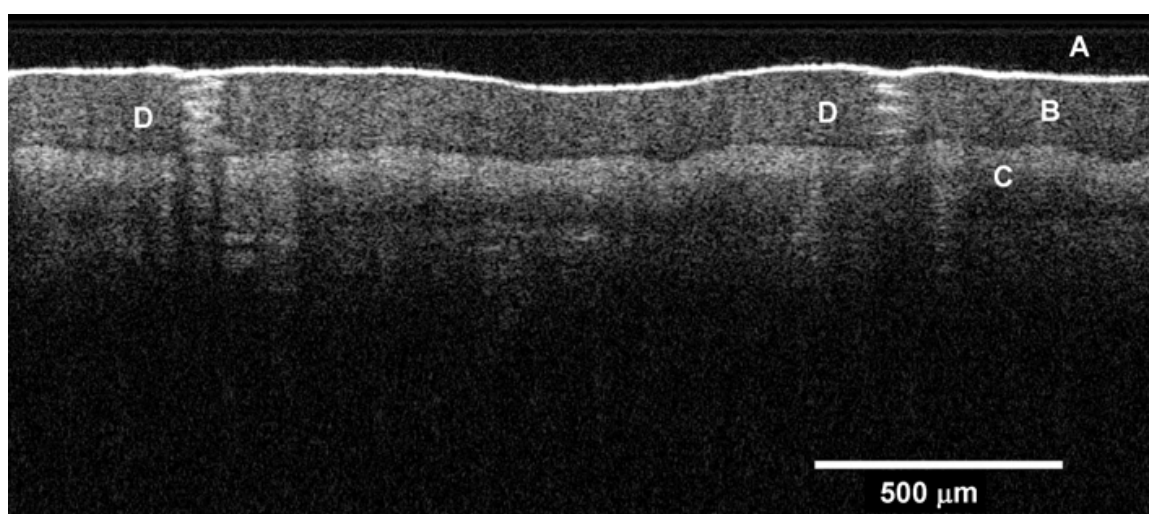

Fig. 1. Optical coherence tomography of a hand palm, the letters indentifies the structures: A) stratum corneum; B) epidermis; C) dermis and D) Sweat gland.

Nowadays OCT is routine in ophthalmologic clinic in many countries (approved by FDA in USA), and is spreading its applications in odontology (Freitas, et al., 2006)(Melo, et al., 2005) dermatology, industrial (Goode, 2008) applications among others. The image, presented in Fig. 1, shows an OCT image of the human hand palm.

The bibliographic data helps to convince the reader about OCT impact and its potential, a brief research was performed in the Web of Science database for the keyword "optical AND coherence AND tomography". Firstly, as shown Fig. 2, the record count, between years 1991 to 2009, has grown consistently since OCT has been proposed and has reached about 1800 documents only in 2009, and only for the keywords inserted in the search engine, for more dramatic comparison, this is 5 documents of OCT per day!
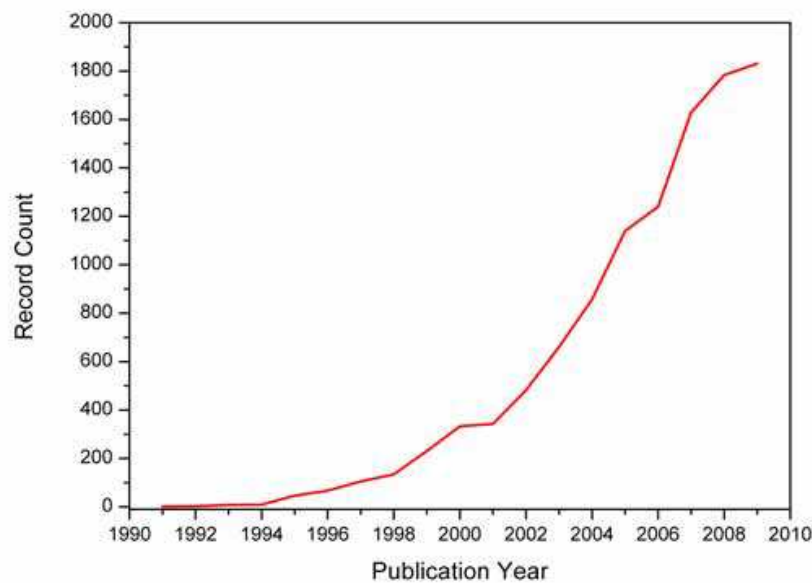

Fig. 2. Record count results for "optical AND coherence AND tomography" keyword in the Web of Science in July of 2010 organized by year.
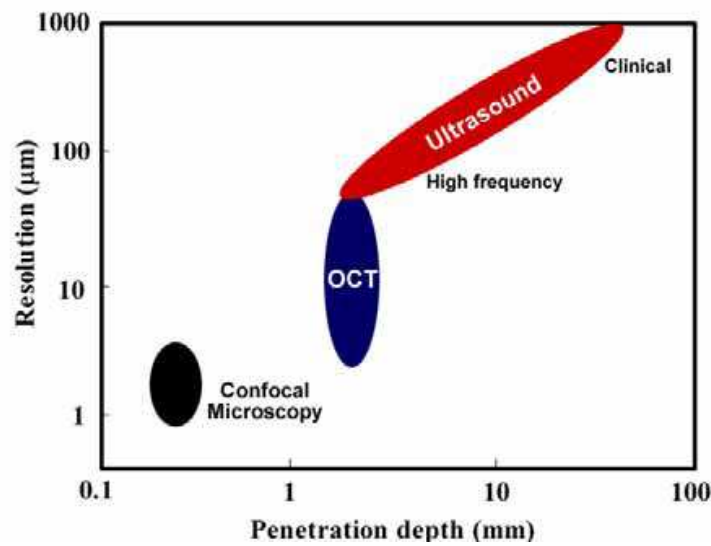

Fig. 3. Regions of actuation of tomographic systems.

These bibliographic productions are classified as shown in the Fig. 4, where worth to mention that patents are the third place in numbers of publications, showing the economic potential of OCT. Another highlight which can be done is about the reviews, this is a way to measure how consolidate a certain technique is, in other words, the expressive number of reviews shows that OCT can be faced as a established imaging tool.

Organizing this data by areas of knowledge and looking only for the most expressive ones, Fig. 5, it is possible to see the impact of OCT in ophthalmology, and also in cardiology, caused by OCT. That is because of the vacancy of technologies capable to perform images with resolution good enough to differ between structures, some of them with few microns sized.
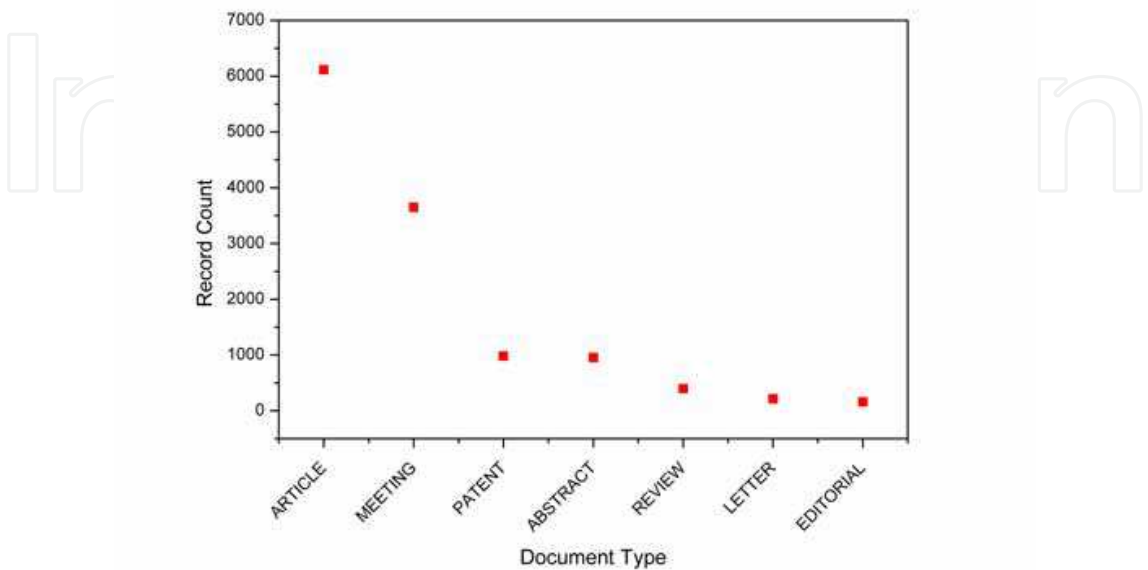

Fig. 4. Record count results for "optical AND coherence AND tomography" keyword in the Web of Science in July of 2010 organized by document type.
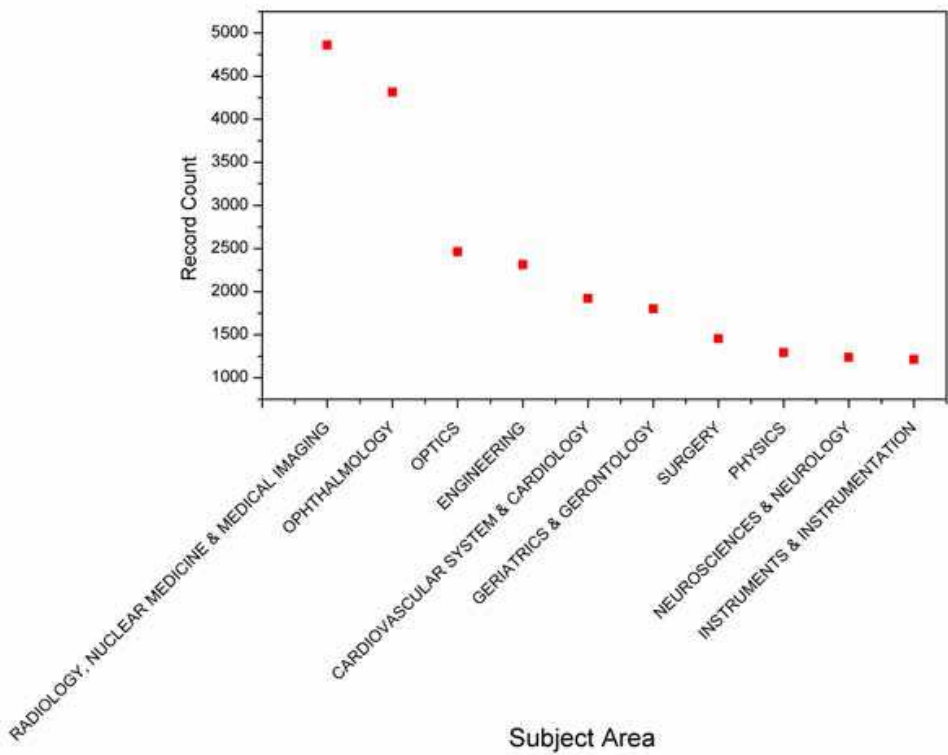

Fig. 5. Record count results for "optical AND coherence AND tomography" keyword in the Web of Science in July of 2010 organized by subject area.

1.1 OCT concept

The OCT setup it is generally mounted with a Michelson interferometer, and can be divided in the following main parts: light source, scanning system and light detector, see Fig. 6. These items define almost all crucial properties of the system. The light emitted from the light source is divided in two by a beam splitter, part of the beam is directed to the sample and the other part to the reference mirror, the light backscattered by the sample and the light reflected by the mirror are recombined at the beam splitter giving origin to an interference pattern collected by the detector. Because the broadband property of the light source, the interference pattern will occur only when the optical paths difference between this two arms are nearly the same. All this process will be discussed in more detail ahead.

The first OCT setup was implemented using femtosecond pulsed laser, due to its broadband spectral emission (Huang, et al., 1991), which implies in a low coherence length, this feature is the heart of the OCT system, and the image resolution is correlated to the light source coherence (as broader the spectral bandwidth, narrower the coherence length will be).
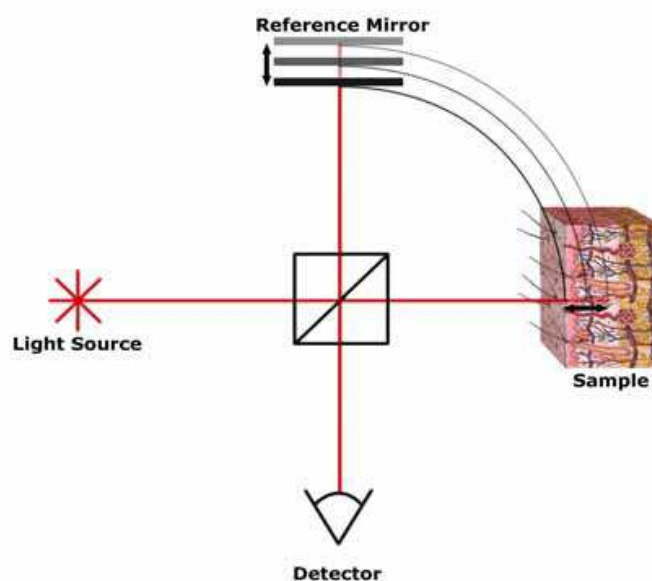

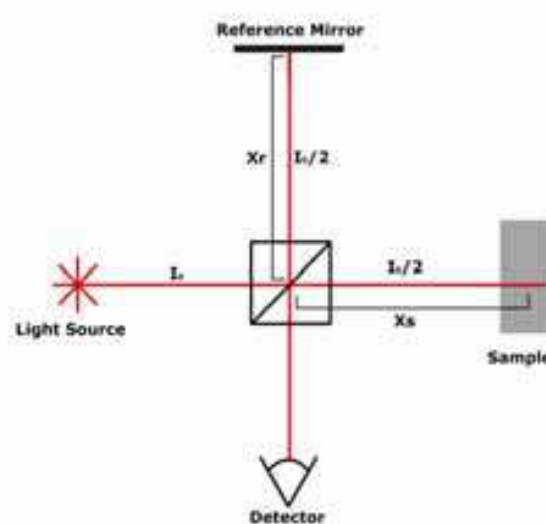Fig. 6. Schematic representation of an OCT setup.

Fig. 7. Michelson Interferometer.

Nowadays many others light properties are explored too, like polarization sensitive OCT or Doppler shift OCT are already established, these techniques can extract information about fiber alignment or particles velocity within the sample, respectively. The efforts by the research groups for other approaches are being done continuously, since the OCT development, resulting in ways to extract more information of the sample by the analysis of the light: Mueller matrix OCT (MM-OCT), pumping-probe OCT (PP-OCT), autocorrelation OCT, are some examples of OCT approaches in current development.

2. Theory

2.1 Low coherence interferometry

The OCT technique is based on Michelson interferometer (Fig. 7) to produce tomographic images. A light source, expressed in terms of it electrical field amplitude (equation (1)) is introduced in the Michelson interferometer and is directed to the beamsplitter. It splits the radiation in two components that are bounded to the reference arm (E_r) and to the sample arm (E_s). Using a beamspliter that divides the beam in two equal parts (50:50), e.g., E_r and E_s can be written as equation (2) and (3) respectively.

$$E_f\left(x\right) = E_{fo}e^{i(kx-\omega t)} \tag{1}$$

using $k = 2\pi / \lambda$, $\omega = 2\pi c / \lambda$ and considering just spatial wave propagation

$$E_S(x) = \left(1/\sqrt{2}\right)E_{fo}e^{i\left(\frac{\omega}{c}x_s\right)} \tag{2}$$

$$E_r(x) = \left(1/\sqrt{2}\right)E_{fo}e^{i\left(\frac{\omega}{c}x_r\right)} \tag{3}$$

The radiation is reflected by the reference mirror, and backscattered by the sample, the portion of radiation that returns is proportional to the mirror and sample capacity to reflect and backscatter this radiation. This coefficient $R(x)$, can vary in sample depth (depending on the sample features). It varies from 0 to 1, where 0 is total transmission and 1 is total reflection. So, the back reflected and backscattered field (light) suffers an amplitude modulation. Moreover, the resultant field will be equal to the sum of infinitesimal fields from different sample depth.

The field comes back to the beamspliter where they are recombined; the field from mirror and sample are described by equation (4) and (5) respectively. For the mirror $R_r(x)=R_r\delta(x-x_0)$, where $\delta(x-x_0)$ is the Dirac function and x_0 is the mirror position.

$$E_r\left(x_r\right) = \left(\frac{1}{2}\right)E_{fo}\int_0^\infty R_r\delta(x_r - x_0)e^{i\left(2\frac{\omega}{c}x_r\right)}dx_r = \left(\frac{1}{2}\right)E_{fo}R_re^{i\left(2\frac{\omega}{c}x_0\right)} \tag{4}$$

$$E_S(x_S) = \left(\frac{1}{2}\right)E_{fo}\int_0^\infty R_S(x_s')e^{i\left(2\frac{\omega}{c}n\left(x_s'\right)x_s\right)}dx_s' \tag{5}$$

The factor two in the exponential is to take in account the optical path roundtrip, $n(x_S)$ is the refraction index as function of sample depth. The electrical field on the detector (E_D) will be a sum of the sample and reference arm electrical fields.

$$E_D = E_r + E_S = \left(\frac{1}{2}\right)E_{fo}R_r e^{i\left(2\frac{\omega}{c}x_0\right)} + \left(\frac{1}{2}\right)E_{fo}\int_0^\infty R_s(x_s)e^{i\left(2\frac{\omega}{c}n(x_s)x_s\right)}dx_s \tag{6}$$

The intensity on detector (I_D) is proportional to square modulus of electrical field E_D:

$$I_D \propto E_D E_D{}^* = \left|\left(\frac{1}{2}\right)E_{fo}R_r e^{i\left(2\frac{\omega}{c}x_0\right)} + \left(\frac{1}{2}\right)E_{fo}\int_0^\infty R_s(x_s)e^{i\left(2\frac{\omega}{c}n(x_s)x_s\right)}dx_s\right|^2 =$$

$$= \left(\frac{E_{fo}}{2}\right)^2 \left[\begin{array}{l} R_r{}^2 + \int_0^\infty \int_0^\infty R_S(x'_S)R_S(x_S)e^{-i\left(2\frac{\omega}{c}\left(n(x_S)x_S - n(x'_S)x'_S\right)\right)}dx_S dx'_S \\ + \left(\int_{-\infty}^\infty R_r R_S(x_S)\cos\left(2\frac{\omega}{c}\left(n(x_S)x_S - x_0\right)\right)dx_S \right) \end{array} \right] \tag{7}$$

At the right side of this equation, the first two terms corresponds to the DC (constant) intensity from reference and sample arm, respectively, and they do not bring useful information. The third term is an oscillatory term, and is responsible of bringing information from the sample to generate OCT images.

Using a broadband spectral source, the equation (7) must be modified in such way that it comprehends an infinity number of frequencies. The interference only occurs between equal frequencies, so the total interference will be the sum of the infinitesimal interferences.

$$I_D \propto \int_0^\infty \left(\frac{E_{fo}(\omega)}{2}\right)^2 \left[\begin{array}{l} R_r{}^2 + \int_0^\infty \int_0^\infty R_S(x'_S)R_S(x_S)e^{-i\left(2\frac{\omega}{c}\left(n(x_S)x_S - n(x'_S)x'_S\right)\right)}dx_S dx'_S + \\ + \left(\int_{-\infty}^\infty R_r R_S(x_S)\cos\left(2\frac{\omega}{c}\left(n(x_S)x_S - x_0\right)\right)dx_S \right) \end{array} \right]d\omega = \int_0^\infty I(\omega)d\omega \tag{8}$$

Where $I_D(\omega)$ is the intensity on detector for a given ω value, and the integral in frequency is equal to the total intensity on detector I_D.

The field that comes from reference and sample arm differs only by the optical path, as expressed by the interference term on equation (7)).

If t is the time that the radiation takes to travel from beamspliter to reference mirror, and $t+\tau$ is the time to travel from beamspliter to the scatter position in the sample, so τ is the temporal delay between the two arms. The interference term on equation (7) can be written as:

$$2\,\mathrm{Re}\,\Gamma_{rS}(\tau) \tag{9}$$

Where,

$$\Gamma_{rS}(\tau) = \left\langle E_r(t)E_S{}^*(t+\tau) \right\rangle_T \tag{10}$$

The $\Gamma_{rS}(\tau)$ is the coherence function or correlation function between E_r and E_S fields. The function:

$$\Gamma_{SS}(\tau) = \left\langle E_S(t)E_S^{*}(t+\tau) \right\rangle_T \tag{11}$$

It is known as autocorrelation function. From this definition it is possible to show that $\Gamma_{SS}(0)=I_S$ and $\Gamma_{rr}(0)=I_r$. For convenience the normalized form of coherence function will be used, it is called partial coherence degree:

$$\gamma_{rS}(\tau) = \frac{\Gamma_{rS}(\tau)}{\sqrt{\Gamma_{rr}(0)\Gamma_{SS}(0)}} = \frac{\Gamma_{rS}(\tau)}{\sqrt{I_r I_S}} \tag{12}$$

The $\gamma_{rS}(\tau)$ function is, in general, a periodic complex function of τ, so the interference pattern is obtained if the value of $|\gamma_{rS}(\tau)|$ is different from zero. The $|\gamma_{rS}(\tau)|$ can assume value between 0 and 1. If the value is equal 1 it says that complete coherence occur, if equal 0 it says that complete incoherence, for values between 0 and 1 partial coherence occurs.

$$|\gamma_{rS}(\tau)| = 1 \qquad \text{Complete coherence} \tag{13}$$

$$0 < |\gamma_{rS}(\tau)| < 1 \qquad \text{Partial coherence} \tag{14}$$

$$|\gamma_{rS}(\tau)| = 0 \qquad \text{Complete incoherence} \tag{15}$$

2.2 Time domain

The Fig. 6 shows the basic components of an OCT system. The main part of the system comprehends an interferometer illuminated by a broadband light source.

The OCT system splits the broadband light source beam in reference field (E_R) and a sample field (E_S). They interfere at the detector by summing up the two electrical fields that are reflected by the optical scanning system (in general a mirror) and the sample. The intensity in the detector can be expressed by equation (8).

The oscillatory term on equation (8) can also be expressed as:

$$\text{Re}\left\{ E_R E_S^{*} \right\} = R_R R_S \cos(2\beta_R l_R - 2\beta_S l_S) \tag{16}$$

Where l is the optical path and β is the propagation constant (in this case the light source is highly coherent).

Defining $S(\omega) = R_S(\omega)R_R(\omega)^*$ and $\Delta\phi(\omega) = 2[\beta_S(\omega)l_S - \beta_R(\omega)l_R]$, and considering the case where the sample and the reference arms consists of a uniform, linear, no dispersive material and the light source spectral density is given by $S(\omega-\omega_0)$, which is considered to be bandwidth limited and centered at the frequency ω_0. The propagation constants $\beta_i(\omega)$ in each arm are assumed to be the same; the diffuse tissue material behaves locally as an ideal mirror leaving the sample beam unchanged. Propagating the $\beta_i(\omega)$ coefficient as a first-order Taylor expansion around the central frequency ω_0 gives

$$\beta_R(\omega) = \beta_S(\omega) = \beta(\omega_0) + \beta^{'}(\omega_0)(\omega - \omega_0) \tag{17}$$

Then the phase mismatch $\Delta\phi(\omega)$ is determined solely by the optical length mismatch $\Delta l = l_S - l_R$ between the reference and the sample arms, and is given by

$$\Delta\phi(\omega) = \beta_0(\omega_0)(2\Delta l) + \beta'(\omega_0)(\omega - \omega_0)(2\Delta l) \tag{18}$$

Now, consider that the light source has a Gaussian power spectral density defined by

$$S(\omega - \omega_0) = \sqrt{\frac{2\pi}{\sigma_\omega^2}} e^{-\frac{(\omega - \omega_0)^2}{\sigma_\omega^2}} \tag{19}$$

which has been normalized to the unit power. Using this power spectrum and the phase mismatch is possible to find that detector signal is:

$$I \propto \frac{e}{h\beta\eta_0} \text{Re}\left\{ \underbrace{1}_{DC} + \underbrace{e^{-\frac{\Delta\tau_g^2}{2\sigma_\tau}} e^{-i\omega_0\Delta_{\tau p}}}_{AC} \right\} \tag{20}$$

In (20), the phase delay mismatch $\Delta_{\tau p}$ and the group delay mismatch $\Delta_{\tau g}$ are defined as:

$$\Delta\tau_p = \frac{\beta(\omega_0)}{\omega_0}(2\Delta l) = \frac{2\Delta l}{v_p} \tag{21}$$

and

$$\Delta\tau_p = \beta'(\omega_0)(2\Delta l) = \frac{2\Delta l}{v_g} \tag{22}$$

The detector signal given by equation (20) contains two terms, the first one is the mean (DC) intensities returning from the reference and sample arms of the interferometer, and the second one, which depends on the optical time delay (optical path mismatch) set by the position of the reference mirror, represents the amplitude of the interference fringes that carry information about the tissue structure, this is a Gaussian envelope with a characteristic standard deviation temporal width $2\sigma_\tau$ that is inversely proportional to the power spectral bandwidth: $2\sigma_\tau = 1/2\sigma_\omega$. This envelope falls off quickly with increasing group delay mismatch $\Delta\tau_g$ and is modulated by interference fringes that oscillate with increasing phase delay mismatch $\Delta\tau_p$. Thus, the second term in equation (20) defines the axial resolving power of the OCT system. For a Gaussian shape function with standard deviation τ, the full width at half maximum (FWHM) is $2\sigma\sqrt{2\ln 2}$ then, the axial resolution of the system is:

$$\Delta l_{FWHM} = \frac{2\ln 2}{\pi} \frac{\lambda_0^2}{\Delta\lambda} \tag{23}$$

where λ_0 is the center wavelength.

2.3 Frequency domain
The Fourier domain optical coherence tomography (FD-OCT) uses a spectrometer, instead a single detector, to analyze the spectral interference pattern (Fig. 8).
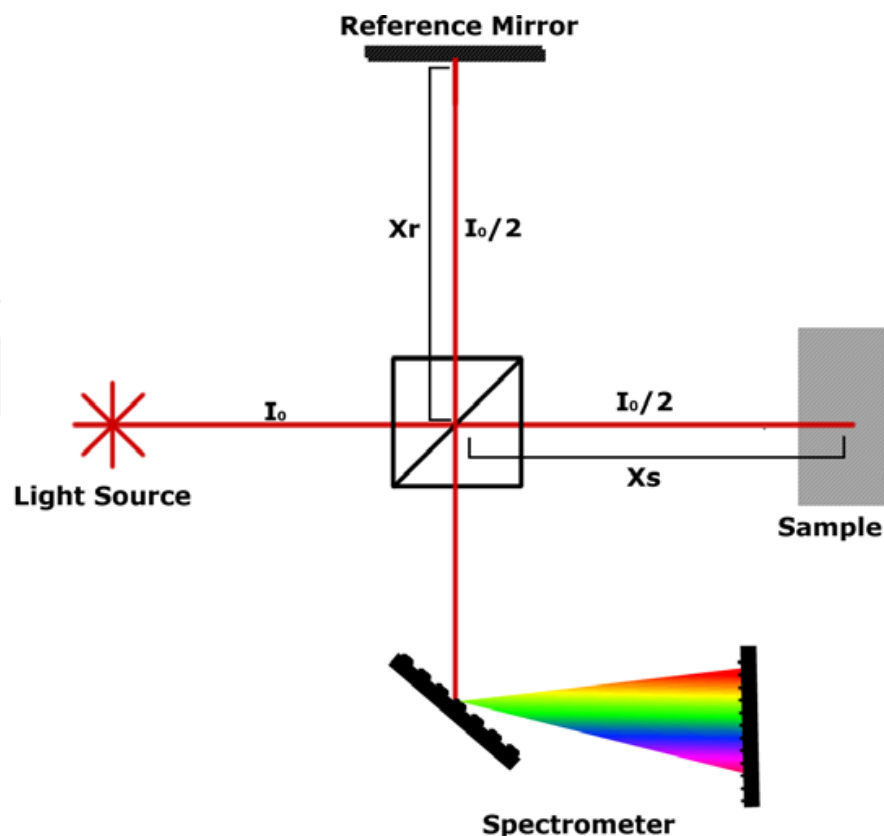
Fig. 8. Michelson Interferometer with a diffractive element an a CCD detector to spectral measurement.

The equation (7) can be written as a Fourier transform of $R_S(x_S)$. To write the equation as a function of wave number k instead ω (equation (24)). There is a correlation between reciprocal and direct space, given by Fourier transform. It correlates time (s) with frequency (1/s=Hz) and distance (m) with wave number k (1/m).

$$I(k) = \left(\frac{E_{fo}(k)}{2} \right)^2 \left[R_r^2 + \int_0^\infty \int_0^\infty R_S(x'_S) R_S(x_S) e^{-i\left(2k\left(n(x_S)x_S - n(x'_S)x'_S\right)\right)} dx_S dx'_S + \frac{1}{2} \Im_z \left[R_r R_S(z) \right] \right] \quad (24)$$

Where $z = n(x_S)x_S - x_0$ is the optical path difference between sample and reference arm. We can also rewrite the second term as a distance related to the reference mirror.

$$\int_0^\infty \int_0^\infty R_S(x'_S) R_S(x_S) e^{-i\left(2\frac{\omega}{c}\left(n(x_S)x_S - n(x'_S)x'_S\right)\right)} dx_S dx'_S$$
$$= \int_0^\infty \int_0^\infty R_S(x'_S) R_S(x_S) e^{-i\left(2k\left[\left(n(x_S)x_S - x_0\right) - \left(n(x'_S)x'_S - x_0\right)\right]\right)} dx_S dx'_S \quad (25)$$

Substituting z in equation (25), and as the auto correlation is a symmetric function, it has:

$$\int_0^\infty \int_0^\infty R_S(z')R_S(z)e^{-i\left(2k[z-z']\right)} dz dz' = \frac{1}{4} \int_{-\infty}^\infty \int_{-\infty}^\infty R_S(z')R_S(z)e^{-i\left(2k[z-z']\right)} dz dz' = \frac{1}{8} \Im_z [AutCorr(R_S(z))]' \quad (26)$$

Can be identified on this term a Fourier transform, using totally reflective mirror in the reference arm (R_r=1), the equation (24) can be rewritten as:

$$I(k) = \left(\frac{E_{fo}(k)}{2}\right)^2 \left(1 + \frac{1}{8}\Im_z[AutCorr(R_S(z))] + \frac{1}{2}\Im_z\left[R_S(z)\right]\right) \tag{27}$$

For the spectral signal (*I(k)*) analysis and *R_S(x_S)* information attainment, an inverse Fourier transform is applied. Finally we obtain:

$$\Im_z^{-1}[I(K)] = \Im_z^{-1}\left[\left(\frac{E_{fo}(k)}{2}\right)^2\right] \otimes \left(\left[\delta(z)\right] + \frac{1}{8}AutCorr(R_S(z)) + \frac{1}{2}R_S(z)\right) \tag{28}$$

$$\Im_z^{-1}[I(K)] = A \otimes (B + C + D) \tag{29}$$

Using a simplified notation (equations (29)) for equation (28), the *R_S(z)* information is present in convolution of A and C (A⊗C). The convolution A⊗B brings information about radiation source properties. A⊗D brings information about interference between waves backscattered in different sample positions. This terms can be ignored for high reflective medium, since this signal is despicable related to A⊗C term. The signal A⊗B and A⊗D can be avoided by adequate reference mirror position, a mismatch of few tens of microns avoid the superposition of A⊗C and the last two terms.

2.3.1 Frequency domain and signal processing
As already discussed in the previous sections, the collected signal in the frequency domain needs to be processed to form images of interest, *i.e.*, processing the signal will make the signal direct related with the sample morphology.
Although the processing algorithm has in the core the Fourier Transform to retrieve the scattering profile (equation (28)), some mathematical manipulations are necessary on the interferometric pattern due to correction and refinements reasons, aiming images with good quality. Some of these corrections are necessary due to physical limitation of the equipment, for example the limited pixel number, or more basic corrections, like changes of unities, for instance.
Many algorithms can be implemented with different approaches, but this text will be focused in just three, they are: Direct Fourier Transform (DirFT), Interpolation (Int) and Zero-Filling (ZF), and they are more detailed explained ahead.
The direct Fourier transform (DirFT) method could be considered as the simpler one, consequently the more fast and robust. It perform just a change of unity, that is because spectrometers are calibrated in wavelength, and as OCTs gives information of depth (m), we need to change from wavelength to wavenumber (*k=2π/λ*). This process makes the spectrum, originally organized in crescent order in wavelength to a reversed order array, so the vector must to be inverted. After that the vector Fourier transform is done, resulting the scattering profile. The schematic diagram represents the process Fig. 9 (a). But this process, *i.e.*, 1/x, cause unequal sized bins, resulting in issues in the Fourier transform, leading to broadening of the structures and asymmetry of the peaks in respect to the it center. A method to avoid this problem is to perform an interpolation. After the changing of unities, the interpolation is done to retrieve equally sized bins, and then submitted to the Fourier transform, this process is schematic represented in the Fig. 9 (b). The last method (Fig. 9 (c)), Zero-Filling (ZF) is a technique more elaborated when compared with the two discussed
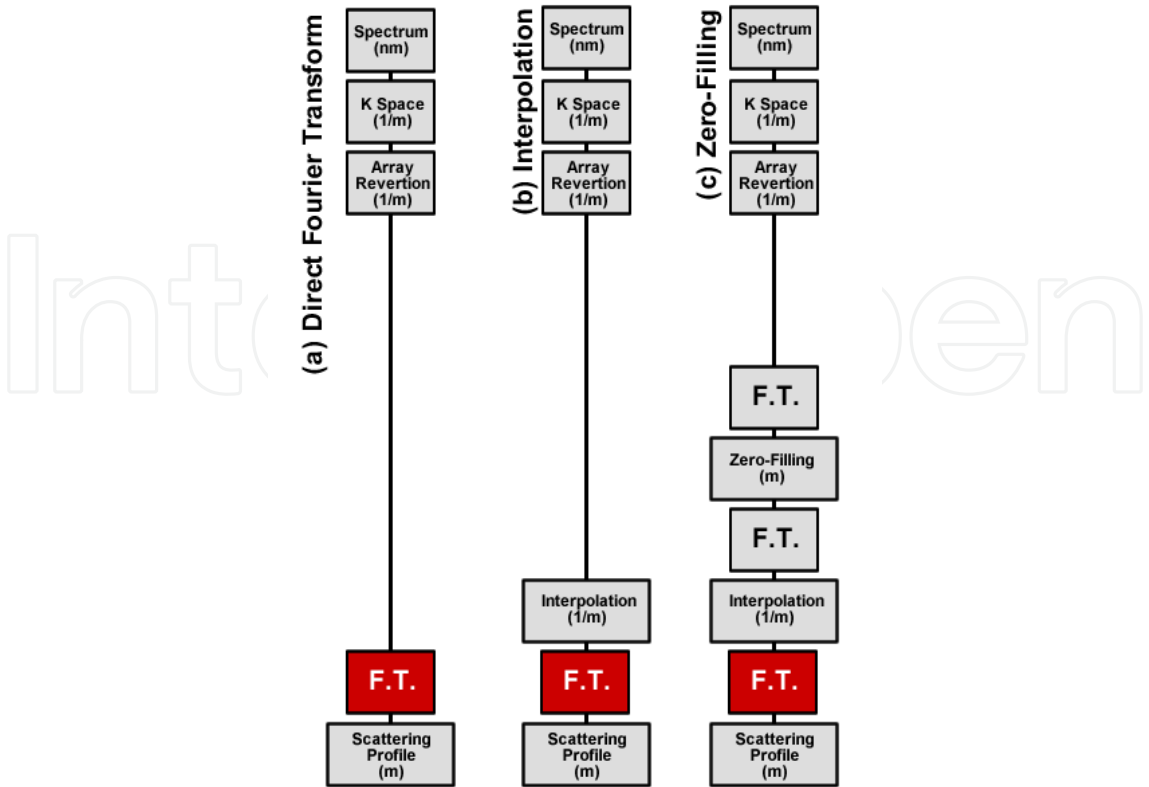
Fig. 9. Schematic representation of three types of spectral interferometry signal processing which results in the scattering profile. Between parenthesis dimensional unity.

previously, consequently more expensive computationally. The Zero-Filling technique is based in a mathematical gimmick, used to increase sampling without increase the data collection. In practice the (ZF) it is preformed applying the Fourier transform on the collected spectrum, then, in the reciprocal space, empty arrays (Zero-Filling) are added at the ends of the original array, the increased sampling of the original data will, according to the Nyquist theorem, allow to process higher frequencies resulting in less computational errors (Raele, et al., 2009).

3. Light source

3.1 Light source characteristics

The light source should attend, basically, four main desired characteristics: wavelength, spectral bandwidth, intensity and stability. Other features could be also listed, as portability, low cost and etc, but these first four are critical and the reasons for that follows.

First of all the wavelength must be compatible with the sample, mainly because scattering, absorption and dispersion are wavelength dependent, so if there is interest in measure inside a sample a wavelength that has low attenuation must be chose. To biological tissue studies, the region known as "diagnostic window" is often used. This spectral region is located between 800 nm and 1300 nm.

As shown by equation (23), the spectral band is related with the system resolution, naturally light sources with broad emission spectral will be preferred, but it is not usual to obtain broad spectral emission with high intensities. Also it is interesting to highlight that to maintain a resolution as the wavelength increases, the spectral band also needs to increases,

for instance an 800 nm with 28 nm of spectral band implies in 10 µm of resolution. To get the same resolution at 1600 nm the spectral band should be 113 nm.

The intensity of the light source must be intense enough to sensitize the detector giving a good signal to noise ratio, but as the OCT is often used in biological samples, the intensities should not overcome the maximum permissible radiation (MPR).

Finally the spectral profile and the intensity must be constant in time; any alteration can cause issues, like false structures, in the scattering image.

3.2 SLED, mode locked lasers, swept sources

Many kinds of light source can be used in OCT systems, as just they fill in the requirements described in the previous section, but let us highlight some features of each one of them.

3.2.1 Super iuminescent LED (SLED)

The SLED it is, perhaps, the most popular OCT light source nowadays due to its low cost and easiness of handling. It presents intensities high enough to perform tomographic images, and also presents high spectral stability. Another good thing about it is that is possible to acquire it pigtailed (connected to an optical fiber). The drawbacks are limited spectral band, about 30 nm and intensities not high enough to perform extremely fast scanning.

3.2.2 Lasers

Lasers, usually, are applied in OCT research, most of them using a Ti:Sapphire laser system operating in mode locked regime, because in this kind of operation a broadband radiation is promoted. Lasers are a most flexible, about spectrum and intensity, then system with SLED. Without doubt the major drawbacks of applying mode locked lasers is the cost.

Lasers systems allows intensities high enough to perform images at so high rates, in this way, the involuntary movements of the live system that are under study do not affect the image.

Mode locked lasers also can be used to generate a supercontinuum spectra by injecting it in a photonic fiber. In this type of fibers, nonlinear effects produces spectra large as 400 nm, allowing submicron of spatial resolutions.

3.2.3 Swept source

A Swept Source is a broadband laser with an intracavity optical narrowband filter. Only longitudinal modes with the exact frequency selected by the filter can oscillate, so the laser action occurs on a single frequency. This filter can be frequency tuned, sweeping the frequency laser action. The filtering tune is made so all the laser spectral frequencies be tuned on the photon cavity roundtrip. The output laser is not a sort pulse train, as a mode-locked laser, but a tuned frequency train with long pulses. The tuned frequencies have the same phase evolution and they are coherent between each other.

4. Scanning systems

Before entering in the subject itself, let us stress to the reader that is more than one type of scanning, usually we need a lateral scan and also a depth scan, be sure that are clear in mind before continue. The lateral scan can be easily done with a galvanometric system or even a

linear translator that moves a sample perpendicularly to the incident light beam. Below are discussed the depth scan, also known as A-scan and have two different approaches to be performed: Time Domain and Frequency Domain, as detailed in the theory section, the issue, now, it is how to perform in practice this two types of A-scan.

4.1 Time Domain

In Time Domain OCT the optical path of the reference arm needs to vary in time so the scattering profile, of a single point of the sample, can be recorded. Change the optical path of an interferometer arm can be done with simple systems, simple as a mirror fixed in a speaker, of course that is not the most reliable and faster way, but it will do. When systems with more finesse are required more complex systems are needed. That are many type of scanning system, when using optical fibers, to stretch it with kHz repetition, usually, can be done using a piezoelectric device. This configuration assures high mechanical stability due to the use of the optical fiber. Another configuration reported is to place a rotating glass cube between the beam splitter and the mirror. As the cube rotates the optical path changes due to refraction, with this setup was achieved the A-scanning record (Bouma, et al., 2002), another used configuration is kwon as Fast Fourier Scanning (FFS) scanning, also achieves high repetition.

4.1.1 Frequency Domain

The main advantage of Frequency Domain OCT it is that, once that a CCD based spectrometer is used, there is no need of any mechanical variation in time. All the depth information, the scattering profile, is encoded in the spectral interference pattern, which can be recorded easily with the help of a personal computer. So in this case the reference arm stands still. In the other hands, as drawbacks about, about the FD-OCT, is the detector cost and complexity, still, is the configuration more used in commercial systems. Another issue to be mentioned is that FD signal needs more processing, i.e., more powerful computers.

4.1.2 Swept source

The swept source can be understood as a characteristic FD approaches, but due to the source features the spectrum is acquired as a function of time. There is a relationship between time and wavelength. Also the signal acquired needs to be processed in the same way that in the FD-OCT. So, what is the catch? Well, now the cost of having a spectrometer is avoided, in SS-OCT a single photo-detector is used (no gratings, no moving mirrors and CCDs). Mechanically the SS setup has no moving parts, as FD, which is a very desirable feature, however, in the SS system the swept source itself it has a high cost and complexity.

The Swept source applied to OCT (SS-OCT) allows images construction between 10 to 50 times quiker than traditional OCT and, due to SS be a laser, the SS intensity is greater than superluminescent LED, allows deeper tissue penetration.

5. PS-OCT

Light exhibits polarization states; due to the property that light vibrates orthogonally in respect to the propagation direction. Measure change in polarization in many cases can be considerate relatively simple process, but measure change in polarization as position function (inside a sample) it is not trivial. Using an OCT system it is possible to gather information from different polarizations states and perform not a scattering image, but it is

possible to perform birefringence images (Hee, et al., 1992). PS-OCT needs some modification in the setup (Fig. 10), a polarized light source a polarization analyzer and a pair of quarter wave plate is needed.
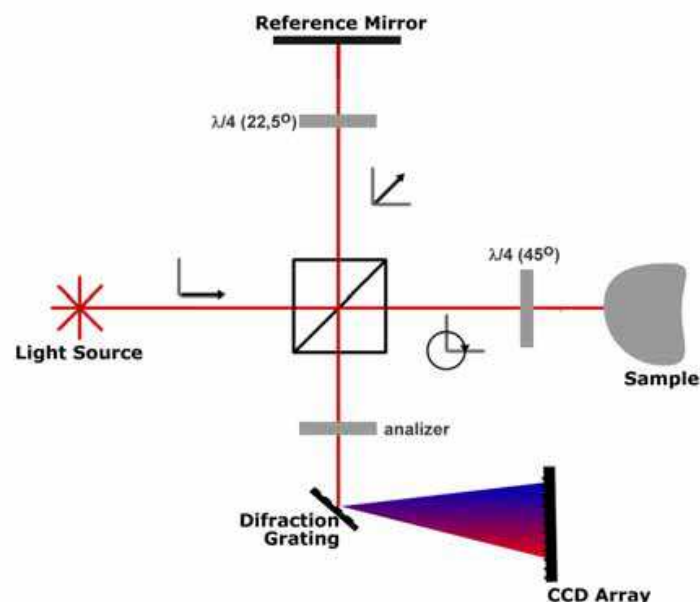

Fig. 10. Diagram to PS-OCT, a linear polarized light is spliced in two parts, in the sample arm the polarization is rotated to 45°, and in the sample arm is converted in circular polarized. The detector register the two orthogonal polarized light depending of the analyzer angle.

The polarized light hits the beam splitter, then a fraction is transmitted and other is reflected. Looking for the sample arm, one can think that the linear polarized light could be aligned with one optical axis of the sample (fast or slow axis) which would result a ordinary OCT scattering image, to avoid that a quarter wave plate, at 45°, is placed before the sample, causing a circular polarization state, in this way the light can be not aligned with any optical axis. The sample will cause some backscattering; the light will then, again, pass through the quarter wave plate. Remembering that the light has passed twice through the quarter wave plate at 45°, the light will return to the beam splitter with a linear polarization state rotated of 90° in respect of the original polarization state (light source).

So in the sample arm the light already contain all the information that is needed, the issue is now on the reference arm, that is because due to the reason that light interfere only when both beams have components of the same polarization state, i.e., a horizontally and a vertically polarized will not interfere, but a horizontally and a 45° polarized light will have a interference because the 45° state of polarization it is a superposition of vertical and horizontal polarization, and in this way will present interference pattern over a DC component. The polarization properties of the light can provide crucial information about the sample structure, and analyzing the polarization properties of a sample by the backscattered light as depth function allow to measure biological tissues and many other materials with strong scattering.

With a Polarization Sensitive OCT birefringence images can be performed (Fig. 11), in this way the differences between the refraction indices can be analyzed as an image, making diagnoses simple to be performed (Raele, et al., 2009).
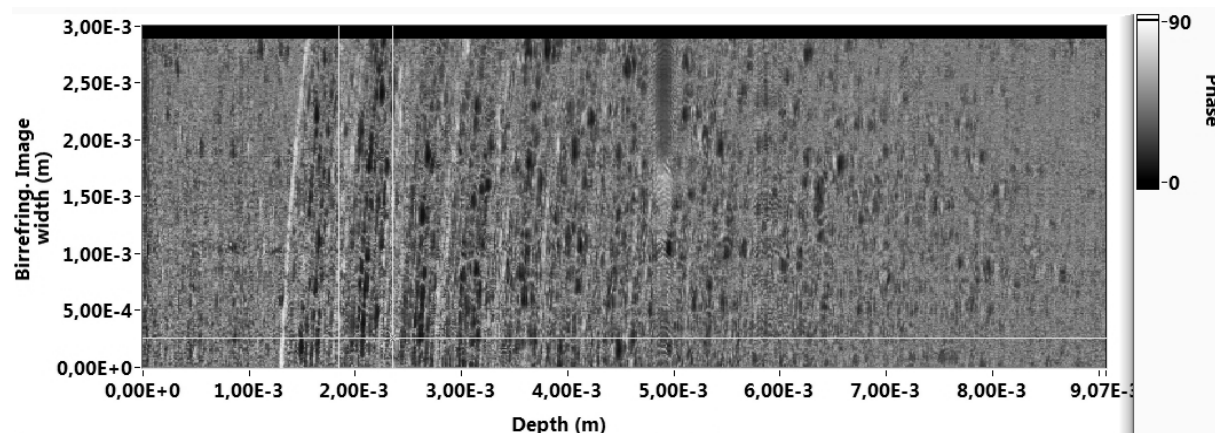
Fig. 11. Birrefringent image with PS-OCT of an adhesive tape, the birefringence of this tape was measured as 4.03(26)x10-4

Besides PS-OCT images, a more complex, but also more complete way to study the polarization properties of light can be done using the Mueller Matrix theory (Bickel, et al., 1985).

5.1 Doppler OCT

A number of extensions of OCT capabilities for functional imaging of tissue physiology have been developed. Doppler OCT (Chen Z, et al., 1997), also named optical Doppler tomography (ODT), combines the Doppler principle with OCT to obtain high-resolution tomographic images of tissue structure and blood flow simultaneously (Fujimoto, et al., 2008). The Doppler OCT combine a technique developed in the 60´s, the Doppler velocimetry, with the traditional OCT high resolution images, mapping the fluids velocity and their localizations in the tissue open a new frontier as a diagnostic tool.

Considering the referential frame moving with a velocity v in this referential the frequency of light will be: $f_0 - \frac{1}{2}\pi K_i \cdot v$ (Fig. 12 (b)), and the scattered light field will be described by:

The light frequency scattered by a moving object will be $2\pi f_0 t - (K_i - K_s) \cdot v$. In a Doppler OCT experiment the light and the scattered light share the same optical path in the sample arm like in (Fig. 12 (a)).

The Doppler shift can be determined measuring the phase shift between two consecutive spectra for A-scan, since in SD-OCT the A-scan are calculated with complex functions (Brezinski, 2006).

$$\tilde{i}_D(z'') = \text{Re}[\tilde{I}_D(z'')] + i Im\left[\tilde{I}_D(z'')\right] = \left|\tilde{i}_D(z'')\right| e^{i\phi(z'')} \tag{30}$$

The phase of this complex function is the phase information of each A-scan described as:

$$\phi(z'') = \arctan\left\{\frac{Im[\tilde{i}_D(z'')]}{Re[\tilde{i}_D(z'')]}\right\} \tag{31}$$

the phase shift $\Delta\phi(z´´)$ can be used to obtain the Doppler velocity.

$$V_D = \frac{\Delta\phi(z'')}{T4\pi k_0 n(k_0)\cos\theta} \tag{32}$$
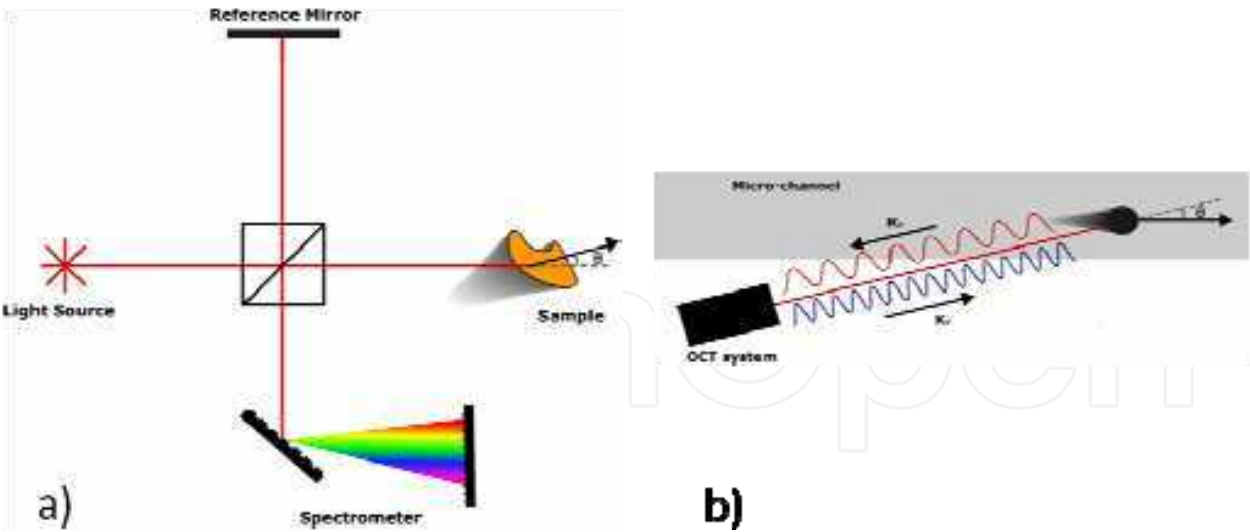
Fig. 12. (a) Diagram of Doppler-OCT and (b) the change in the wavelength of scattered light from a moving particle

6. Applications

6.1 Ophthalmology

OCT systems found it first application performing retina tomographies (Huang, et al., 1991), this was the beginning of what have become a revolution in the ophthalmology area, OCT allowed the specialists to exams the eye as the same way of histology does, but in a completely non invasive, non traumatic and painless way and also in real time. Latter OCT image resolution and depth characteristics matches the needs of ophthalmologists and the eye itself, especially when the OCT is operating at the NIR region, which has low attenuation and does not sensibilizes the vision cells. Besides retina the specialists also use OCT to examine the eye anterior segment and cornea, see Fig. 13. Nowadays OCT is routine in many ophthalmic clinics around the world, and researches are improving this tool continuously.

Diseases as glaucoma and retinal dystrophy among many other examples (Schuman, et al., 2004) can be diagnosed using OCT systems, some of them were a complicated issue to diagnoses, as macular degeneration, has now the OCT as a primary way to do it.
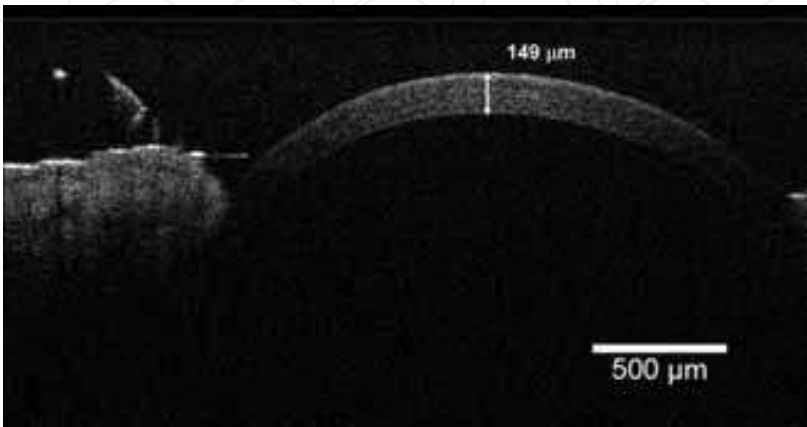

Fig. 13. Image of a mice cornea. The arrow indicates the place where a thickness of it was evaluated.

In terms OCT improvements, some outstanding studies has being done, for instance reported 3 μm of resolution (Wampler), this is refined enough to actually "see" the retina cells. The possibilities of applications are many, monitoring LASIK proceedings, study the blood flux, etc.

6.2 Dermatology

OCT also caused a significant impact dermatology for almost the same reasons that promoted OCT in ophthalmology. As shown in Fig. 1, OCT technique can perform images where is possible to indentify the different skin structures (A. stratum corneum; B. epidermis; C. dermis and D. Sweat gland), researches are studing many features of skin *in vivo*, impossible feat before OCT.

Diseases, even skin cancer, can be diagnosed by this tool (Mogensen, et al., 2009). Skin has been studied extensively also with PS-OCT (Hee, et al., 1992), that is because many compounds in skin presents birrefringence and the concentration of this compounds are related with skin health.

6.3 Odontology

In odontology, a series of reports first appeared (Colston, et al., 1998), (Feldchtein, et al., 1998) in 1998, with imaging of both hard and soft oral tissues. This led to several diagnostics of bucal diseases, including periodontal, early caries, among others. Another area in dentistry where OCT can have important findings is in dental restoration imaging.(Wang, et al., 1999), (Fried, et al., 2002), (Otis, et al., 2000), (Jones, et al., 2004), (Wang, et al., 1999) and (Fried, et al., 2002) exploited polarization-sensitive OCT to identify dental tissue/restoration interfaces. To date, there is no quantitative method capable to perform *in vitro* or *in vivo* analysis of dental restoration, particularly from the clinical point of view. Visual inspection and X-ray imaging are not precise enough to diagnose small gaps that result from bad restoration procedures. Dental tissues are high scattering media and infrared light can penetrate the full enamel extension (Fried, et al., 1995).

Although, in odontology, OCT is not yet broadly available, as in ophthalmology, the potential of the technique promises a fast technological development that requires more laboratory evaluation, prior to clinical trials.

One of important area of interest is the restorative procedures, the application of OCT to dental restoration, particularly analyzing failure gaps left after the restoration has been performed (Melo, et al., 2005).

Another import field of interest is the dental caries, and this disease is known as a multifactorial pathological process, characterized by hard tissue demineralization. Commonly, dentists evaluate the oral health of a patient through three main methods: visual, tactile examination and radiographic imaging (Bosh, 1993). The visual method cannot detect early caries lesion and depends of the dentist ability to identify these lesions. There are many caries detector dyes commercially available purported to assist the dentist in differentiation of infected tissue, but they are not specific and would result in unnecessary removal of healthy tooth structure (McComb, 2000). OCT in dentistry has been recently used to in vitro studies evaluating enamel interface restoration (Melo, et al., 2005), early caries diagnostics (Freitas, et al., 2006), and analysis of the performance of dental materials (Braz, et al., 2009). In 2006, the first OCT image of dental pulp was performed using rat's teeth (Kauffman, et al., 2006), and more recently, remaining dentin and pulp chamber from human's teeth were also imaged by OCT in vitro (Fonseca, et al., 2009).

The OCT can detect and quantify demineralization (FREITAS, et al., 2009). The Fig. 14 (a) shows an OCT image for a sample submitted to the demineralization process for 11 days, and in (b) the 3D image reconstruction.

The OCT system provides a powerful contact less and noninvasive diagnostic method that could be used to complement the traditional diagnostic methods such as X-ray radiography, avoiding potentially hazardous ionization radiation.

Polarization-sensitive optical coherence tomography (PS-OCT) is potentially useful for imaging the nonsurgical remineralization of dental enamel. The PS-OCT can image the effects of mineralization status and scattering properties of dental caries (Jones, et al., 2006), (Baumgartner A, et al., 2000).
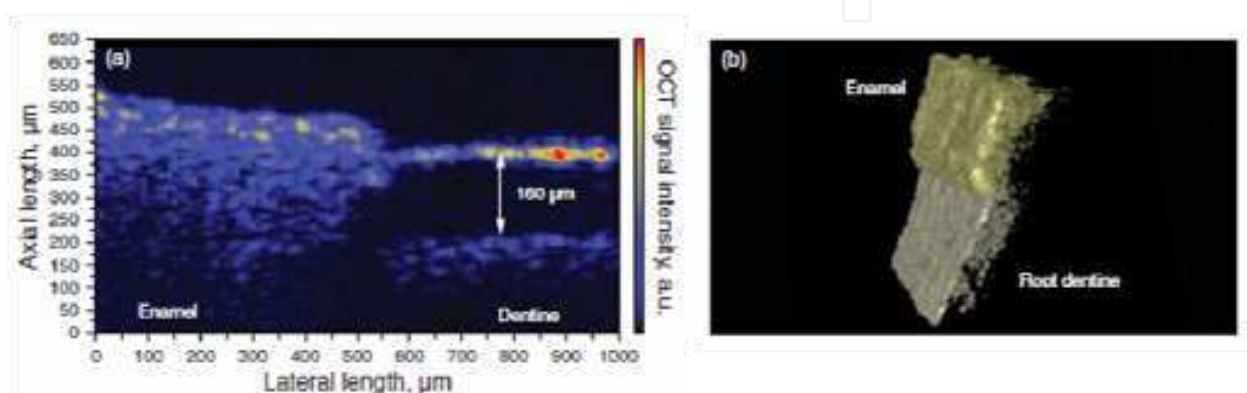

Fig. 14. (a) Transversal OCT image after the sample was submitted to the demineralization process for 11 days and (b) 3D image reconstruction allows another image sections analysis different from those obtained directly from the OCT system.

6.4 Non-biomedical applications

Despite the wide use of OCT for biological application, it noninvasive and nondestructive features are very attractive in other areas. The use of OCT technique has grown on art and cultural heritage artifacts studies (Targowski, et al., 2006) (Liang, et al.), e.g., for investigate various art objects such as oil paintings, see Fig. 15 and Fig. 16, on canvas to image pigments, glaze and varnish layers (Rouba, et al., 2008) or historical coins (Amaral, et al., 2009) for instance.
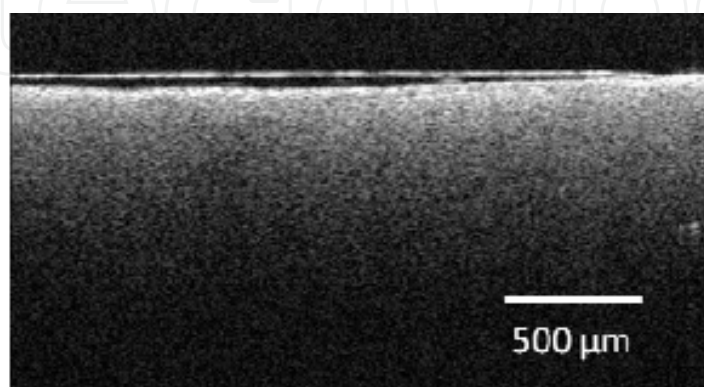

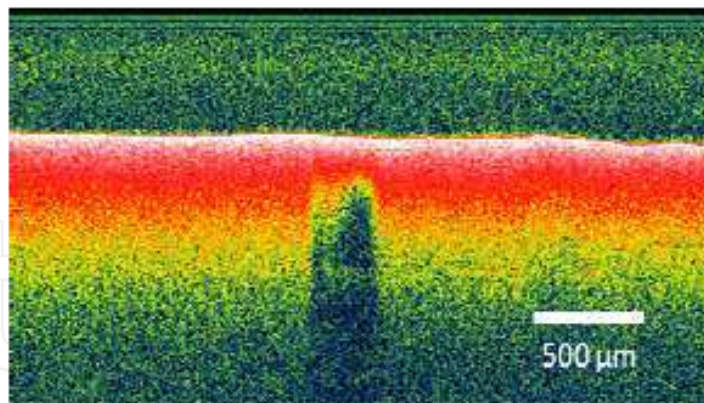Fig. 15. Image of oil painting with varnish layer

Fig. 16. Image of oil painting over sketch made with pencil.

It has been also used also for investigate wood from musical instruments structures, as fibers, rays, cell wall distribution. As well as varnished wood: morphological properties, such roughness, interfaces, and thickness; and compositional properties, such shape, size, distribution of pigments and fillers. And even more, understanding of the penetration of the varnish inside the wood or the wear processes of these materials, applying these kinds of study on a 18th century Italian violin (Latour, et al., 2009).

OCT finds on industry another field of actuation, due to the real time and noncontact feature. Moreover, some traditional technique, used in the industry, cannot be applied to some materials. For e.g., to measure textile roughness, see Fig. 17, traditional technique to roughness measurement, that uses contact cantilever, could cause erroneous values and even damage the textile. Is reported the development of a methodology and algorithm to give metrological parameter of roughness according DIN4768 (Amaral, et al., 2009), that can be applied to delicate samples. Applications also can be found in printed electronics products quality (Czajkowski, et al., 2010) and in paper industry (Prykär, et al., 2010).
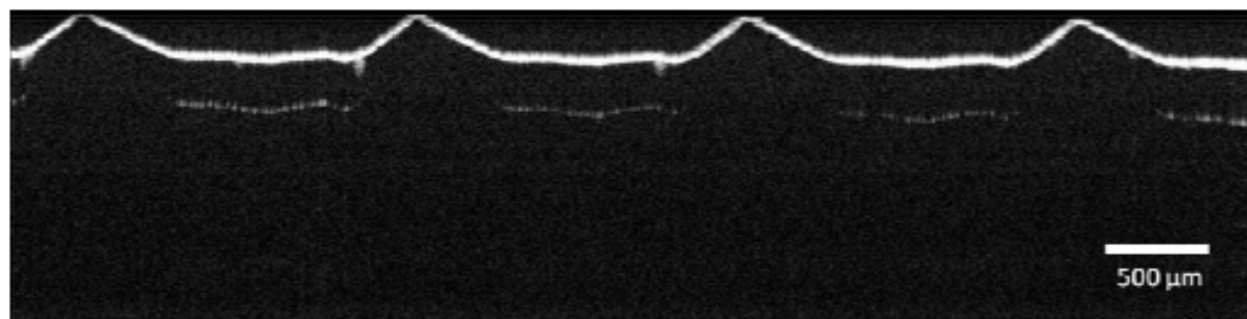

Fig. 17. OCT images can be used to perform roughness measurements without contact.

6.5 Dermatology

OCT also caused a significant impact dermatology for almost the same reasons that promoted OCT in ophthalmology. As shown in Fig. 1, OCT technique can perform images where is possible to indentify the different skin structures, researches are studing many features of skin *in vivo*, impossible feat before OCT.

Diseases, even skin cancer, can be diagnosed by this tool (Mogensen, et al., 2009). Skin has been studied extensively also with PS-OCT (Hee, et al., 1992), that is because many compounds in skin presents birrefringence and the concentration of this compounds are related with skin health.

Another important subject in dermatology is cosmetic science, which claim for a non invasive method to efficiency evaluation of anti-aging or anti-wrinkle products, for instance. Hair is a substructure of skin and it also can be studied with OCT. Fig. 18 (a) shows the cross-sectional image of Afro-Ethnic hair, where is possible to identify two hair structures: medulla and cortex (Lademann, et al., 2008), (Velasco, et al., 2009). The tridimensional image (Fig. 18 (b) was built starting from 601 cross-sectional images (slices) like Fig. 18 (a).
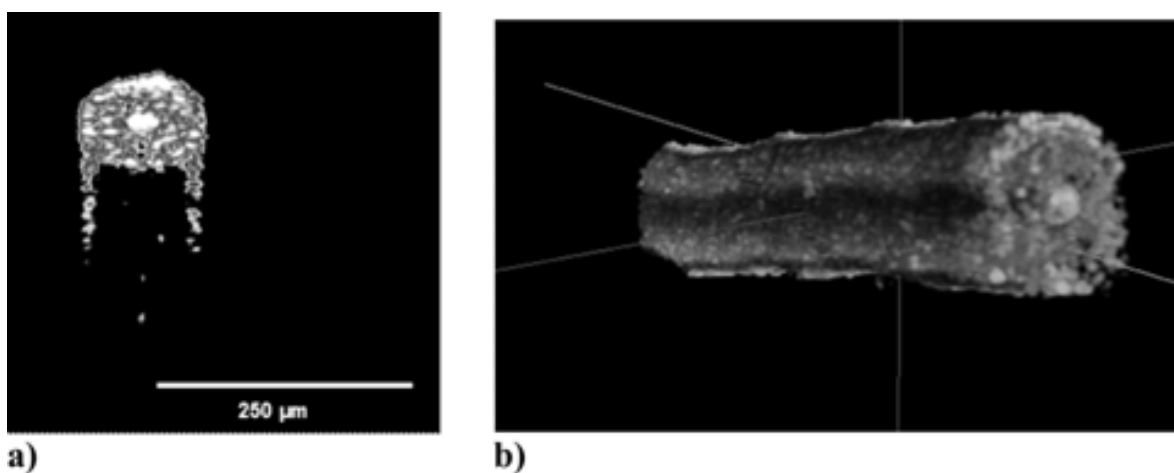

Fig. 18. OCT image of an Afro-Ethnic hair sample. In (a) a sample of cross-section fiber and at (b) a tridimensional reconstruction of that fiber, showing the main hair structures: medulla, cortex and cuticle.

8. Conclusions

Using broadband light sources, as mode locked lasers, in an interferometric setup allows perform tomographic images with high resolution and non invasive way. This technique, known as optical coherence tomography (OCT), found, in many areas of knowledge, great potential. Worth mention that in ophthalmology OCT promoted a revolution in the way that diagnoses are performed.

Although OCT is a relatively new technique, created in 1991, the applications and more powerful and versatile systems are increasing rapidly in number.

9. References

A Baumgartner [et al.] Polarization–Sensitive Optical Coherence Tomography of Dental Structures [Artikel] // Caries. Res.. - 2000 . - Bd. 34.

Amaral Marcello M. [et al.] "Roughness measurement methodology according to DIN 4768 using optical coherence tomography (OCT) [Konferenz] // Proc. SPIE. - Munch : Spie, 2009. - Bd. 7390.

Amaral Marcello M. [et al.] Laser induced breakdown spectroscopy (LIBS) applied to stratigrafic elemental analysis and optical coherence tomography tomography (OCT) to damage determination of cultural heritage Brazilian coins [Konferenz] // Proc. SPIE / Hrsg. Spie. - Munch: Spie, 2009. - Bd. 7391.

Andrew M. Rollins Siavash Yazdanfar, Jennifer K. Barton, Joseph A. Izatt, " Real-time in vivo color Doppler optical coherence tomography [Artikel] // J. Biomed. Opt.. - 2002. - S. Vol. 7, 123.

Baumgartner A Dichtl S, Hitzenberger C K [et al.] Polarization–Sensitive Optical Coherence Tomography of Dental Structures [Artikel] // Caries. Res.. - 2000. - Bd. 34. - S. 59-69.

Bickel W.S. und Bailey W.M. Stokes vectors, Mueller matrices, and polarized scattered light [Artikel] // Am. J. of Phys.. - 1985. - S. v.53, n,5, p. 468-478.

Bosh B. Angmar-Mansson and J.J. Ten Optical Methods for the Detection and Quantification of Caries [Artikel] // Adv. Dent. Res. - 1993. - Bd. 7. - S. 70–79 .

Bouma Brett E. und Tearney Guillermo J. Handbook of Optical Coherence Tomography [Buch]. - NY : Marcel dekker Inc, 2002.

Braz A.K.S. [et al.] Evaluation of crack propagation in dental composites by optical coherence tomography [Artikel] // Dent. Mater.. - 2009. - Bd. 25. - S. 74-79.

Brezinski Mark E. Optical Coherence Tomography, Principles and Applications [Buch]. - Oxford : Elsevier Inc., 2006.

Chen Z Milner T, Dave D und Nelson [Artikel] // J. Opt. Lett.. - 1997. - S. 22 64–6.

Colston B. W. [et al.] Dental OCT [Artikel] // Opt. Express. - 1998. - Bd. 3. - S. 230-238.

Colston B. W. [et al.] Imaging of hard-and soft-tissue structure in the oral cavity by optical coherence tomography [Artikel] // Appl. Opt.. - 1998. - Bd. 37.

Czajkowski Jakub [et al.] Optical coherence tomography as a method of quality inspection for printed electronics products [Artikel] // Opt.l Review. - 2010. - 3 : Bd. 17. - S. 257-262.

Eden Alec The search for Christian Doppler [Buch]. - Wien : Springer-Verlag, 1992.

Feldchtein F. I. [et al.] In vivo OCT imaging of hard and soft tissue of the oral cavity [Artikel] // Opt. Express. - 1998. - Bd. 3. - S. 239-250.

Fercher A. F. [et al.] In vivo optical coherence tomography [Artikel] // Amer. J. Ophthalmol.. - 1993. - S. v.116, pp. 113-114,.

Fonseca D.D.D. [et al.] [Artikel] // J. Biomed. Opt.. - 2009. - Bd. 14. - S. 024009.

Freitas A. Z. [et al.] Imaging carious human dental tissue with optical coherence tomography [Artikel] // J. Appl. Physics. - 2006. - 024906 : Bd. 99.

FREITAS A.Z. [et al.] Determination of dental decay rates with optical coherence tomography [Artikel] // Laser Physics Letters. - 2009. - Bd. 6. - S. 896-900.

Freitas A.Z. [et al.] Imaging Carious Human Dental Tissue with Optical Coherence Tomography [Artikel] // Journal of Applied Physics. - 2006. - S. v. 99, n.2, p.24906.

Fried D. [et al.] Nature of light scattering in dental enamel and dentin at visible and nearinfrared wavelengths [Artikel] // Appl. Opt.. - 1995. - Bd. 34. - S. 1278-1285.

Fried D., Shafi S. und Featherstone J. D. B. Imaging caries lesions and lesion with polarization sensitive optical coherence tomography [Artikel] // J. Biomed. Opt.. - 2002. - Bd. 7. - S. 618–626.

Fujimoto J. G. und Drexler W. Optical Coherence Tomography [Buchabschnitt]. - Berlin : Springer, 2008.

Goode B.G. Optical Coherence Tomography: OCT aims for Industrial Applications [Online]. - 10. 9 2008. - 10. 9 2008. – http://www.laserfocusworld.com/display_article/368547/12/none/none/Feat/ OPTICAL-COHERENCE-TOMOGRAPHY:-OCT-aims-for-industrial-application.

Hee M. R. [et al.] Polarization-sensitive low-coherence reflectometer for birefringence characterization and ranging [Artikel] // J. Opt. Soc. Am B. - 1992. - S. v. 9, p. 903-908.

Hee M.R. [et al.] Optical coherence tomography of the human retina [Artikel] // Arch. Ophthalmol.. - 1995. - S. Vol. 113, pp.326-332.

Huang D. [et al.] Optical Coherence Tomography [Artikel] // Science. - 1991. - 1178 : Bd. 254.

J. Wang T. E. Milner, and J. S. Nelson Characterization of fluid flow velocity by optical Doppler tomography [Artikel] // OPTICS LETTERS. - 1995. - S. Vol. 20, No. 11 / 1337-1339.

Jones R. S., Staninec M. und Fried D. Imaging artificial caries under composite sealants and restorations [Artikel] // J. Biomed. Opt.. - 2004. - Bd. 9. - S. 1297–1304 .

Jones Robert S. [et al.] Remineralization of in vitro dental caries assessed with polarization-sensitive optical coherence tomography [Artikel] // Journal of Biomedical Optics. - 2006. - 1 : Bd. 11. - S. 014016.

Jones Robert S. [et al.] Remineralization of in vitro dental caries assessed with polarization-sensitive optical coherence tomography [Artikel] // Journal of Biomedical Optics. - 2006. - 1 : Bd. 11.

Kato I. T. [et al.] Inhibition of enamel remineralization with blue LED: an in vitro study [Konferenz] // Proc. of Spie Lasers in Dentistry XV. - San José : Spie, 2009. - S. v. 7162.

Kauffman C.M.F. [et al.] [Konferenz]. - [s.l.] : Proc. SPIE, 2006. - 613707 .

Lademann J. [et al.] Application of optical non-invasive methods in skin physiology [Artikel] // Laser Phys. Lett.. - 2008. - 5 : Bd. 5. - S. 335-346.

Latour Gaël [et al.] Structural and optical properties of wood and wood finishes studied using optical coherence tomography: application to an 18th century Italian violin [Artikel] // Applied Optics. - 2009. - 33 : Bd. 48. - S. 6485-6491 .

Liang Haida [et al.] 2. En-face optical coherence tomography: a novel application of non-invasive imaging to art conservation [Artikel] // Optics Express. - 16 : Bd. 13. - S. 6133-6144 .

Martinez O. E. 3000 times grating compressor with positive group velocity dispersion: Application to fiber compensation in 1.3-1.6 pm regime [Artikel] // O. E. Martinez, IEEE J. Quantum Electron. QE-23, 59 (1987).. - 1987. - Bde. QE-23.

McComb D. Diagnoses of occlusal caries [Artikel] // J. Can. Dent. Assoc.. - 2000. - Bd. 66. - S. 195–198 .

Meirelles R.L., Aggio F.B. und Costa R.A. STRATUS optical coherence tomography in unilateral colobomatous excavation of the optic disc and secondary retinoschisis [Artikel] // Graefes Archive For Clinical And Experimental Ophthalmology. - 2005. - S. V. 243, n. 1, p. 76-81.

Melo L. S. A. [et al.] Evaluation of enamel dental restoration interface by optical coherence tomography [Artikel] // Journal of Biomedical Optics. - 2005. - S. v.10, n.6, p.1-5.

Mogensen Mette [et al.] OCT imaging of skin cancer and other dermatological diseases [Artikel] // Journal of Biophotonics. - 2009. - 6-7: Bd. 2. - S. 442 - 451.

Otis L. L. [et al.] Identification of occlusal sealants using optical coherence tomography [Artikel] // J. Clin. Dent.. - 2000. - Bd. 14. - S. 7–10.

Prykär Tuukka [et al.] Optical coherence tomography as an accurate inspection and quality evaluation technique in paper industry [Artikel] // Opt. Review. - 2010. - 3 : Bd. 17. - S. 218-222.

Raele Marcus Paulo and Freitas Anderson Zanardi Desenvolvimento de um sistema de tomografia por coerência óptica no domínio de Fourier sinsível á polarização e sua utilização na determinação das matrizes de Mueller [Report]. - São Paulo : Instituto de Pesquisas Energéticas e Nucleares IPEN-CNEN/SP, 2009.

Rouba Bogumiła J. [et al.] Optical coherence tomography for non-destructive investigations of structure of objects of art [Konferenz] // 9th International Conference on NDT of Art. - Jerusalem : [s.n.], 2008 .

Schuman Joel S., Puliafito Carmen A. and Fujimoto James G. Optical Coherence Tomography of Ocular Diseases [Book]. - NJ : SLACK, 2004.

Shuliang J., Gang Y. und Lihong Depth-resolved two-dimensional Stokes vectors of backscattered light and Mueller matrices of biological tissue measured with optical coherence tomography [Artikel] // Appl. Opt.. - 2000. - S. v. 39, n. 34, p. 6318-6324.

Targowski Piotr, Góra Michalina und Wojtkowski Maciej Optical Coherence Tomography for Artwork Diagnostics [Artikel] // Laser Chemistry. - 2006. - Bd. 2006.

Tearney G. J., Bouma B. E. und Fujimoto J. G. High-speed phase- and group-delay scanning with a grating-based phase control delay line [Artikel] // Opt. Lett.. - 1997. - Bd. 22.

Velasco Maria Valéria Robles [et al.] Prospective ultramorphological characterization of human hair by optical coherence tomography [Artikel] // Skin Research and Technology. - 2009. - Bd. 15. - S. 440-443.

Wampler Steve OCT News [Online] // OCT News. - 30. 07 2010. – https://publicaffairs.llnl.gov/news/news_releases/2010/NR-10-07-02.html.

Wang X. J. [et al.] Characterization of dentin and enamel by use of optical coherence tomography," , () [Artikel] // Appl. Opt.. - 1999. - Bd. 38. - S. 2092–2096.

Web of Science [Online] // Web of Science. - 7 2010, 7. – http://www.isiknowledge.com/WOS.

Zhongping Chen Thomas E. Milner, Digant Dave. und Nelson J. Stuart Optical Doppler tomographic imaging of fluid flow velocity in highly scattering media [Artikel] // Optics Letters. - 1997. - S. Vol. 22, Issue 1, pp. 64-66.

Zhongping Chen Thomas E. Milner, Shyam Srinivas, Xiaojun Wang, Arash Malekafzali, Martin J. C. van Gemert, and J. Stuart Nelson Noninvasive imaging of in vivo blood flow velocity using optical Doppler tomography [Artikel] // Optics Letters. - 1997. - S. Vol. 22, Issue 14, pp. 1.

Laser Pulse Phenomena and Applications

Edited by Dr. F. J. Duarte

Pulsed lasers are available in the gas, liquid, and the solid state. These lasers are also enormously versatile in their output characteristics yielding emission from very large energy pulses to very high peak-power pulses. Pulsed lasers are equally versatile in their spectral characteristics. This volume includes an impressive array of current research on pulsed laser phenomena and applications. *Laser Pulse Phenomena and Applications* covers a wide range of topics from laser powered orbital launchers, and laser rocket engines, to laser-matter interactions, detector and sensor laser technology, laser ablation, and biological applications.

How to reference

In order to correctly reference this scholarly work, feel free to copy and paste the following:

Anderson Freitas, Marcello Amaral and Marcus Raele (2010). Optical Coherence Tomography: Development and Applications, Laser Pulse Phenomena and Applications, Dr. F. J. Duarte (Ed.), ISBN: 978-953-307-405-4, InTech, Available from: http://www.intechopen.com/books/laser-pulse-phenomena-and-applications/optical-coherence-tomography-development-and-applications

INTECH
open science | open minds